NUMERICAL SIMULATION ON THE SEISMIC PERFORMANCE OF PC UTILITY POLES ON SHINKANSEN VIADUCT USING AEM AND FEM

Thanh Ngoc Phan[1,2]*, Akira Hosoda[3], Hamed Salem[4], Mikihisa Yamada[5]

[1]*The University of Danang - University of Technology and Education, Vietnam*
[2]*Institute for Multidisciplinary Sciences, Yokohama National University, Japan*
[3]*Institute of Urban Innovation, Yokohama National University, Japan*
[4]*Structural Engineering Department, Cairo University, Egypt*
[5]*Graduate School of Urban Innovation, Yokohama National University, Japan*

*Corresponding author: ptngoc@ute.udn.vn

(Received: September 26, 2024; Revised: October 11, 2024; Accepted: October 12, 2024)

DOI: 10.31130/ud-jst.2024.529E

Abstract - The 2011 Tohoku earthquake caused severe damage to various infrastructures in the Tohoku region of Japan. Particularly, prestressed concrete (PC) utility poles on Shinkansen viaducts sustained significant damage, leading to prolonged service disruptions. To better understand the structural behavior and failure mechanisms of these poles, JR East company initiated a series of experimental investigations to examine their bending capacity and failure modes under cyclic loading. This research aims to numerically simulate the performance of the tested PC utility poles using Applied Element Method (AEM) and Finite Element Method (FEM). The simulation results demonstrate that both AEM and FEM effectively reproduce the load-displacement relationship observed in the test. Additionally, this study discusses the material models employed in simulations, considering the limitations inherent in numerical modeling. The findings provide critical insights into the structural performance of the poles under seismic loading and offer useful numerical tools for the development of retrofitting strategies.

Key words - Applied Element Method; Finite Element Method; prestressed concrete utility poles; seismic resistance

1. Introduction

The 2011 Great East Japan earthquake characterized by its high magnitude and long duration, caused severe damage to various infrastructures, including railway systems in the Tohoku region of Japan [1]. In particular, prestressed concrete (PC) utility poles on Shinkansen viaducts sustained significant damage, leading to prolonged service disruptions, as shown in Figure 1 [2]. According to a technical report, the failure of PC poles was categorized into two main groups including breakage damage near the footing due to crushing and spalling of concrete (Figure 2a) and inclination of the poles (Figure 2b) [2].

After the event of Tohoku earthquake in 2011, the seismic design code for railway structures was revised in 2012 and followed by seismic design guidelines in 2013 [3]. As for the existing PC utility poles, several conventional retrofitting methods were proposed and practically applied [1, 2, 4]. However, due to the large time consumption for the construction of these methods while the retrofitting plan for about 8,000 poles was fixed by the East Japan Railway Company (JR East) from 2023 to 2033, there is a need to develop a new method which can be easily installed within a short period of time. Therefore, to better understand the structural behavior and failure mechanisms of these PC utility poles, JR East initiated a series of experimental investigations to examine their bending capacity and failure modes under cyclic loading [4].

Figure 1. *Damage of PC utility poles on Shinkansen viaduct [2]*

a) Example of breakage b) Example of inclination

Figure 2. *Examples of damage types [2]*

Due to the limited numerical analysis studies in this field, the current research aims to numerically simulate the performance of the tested PC utility poles using the Applied Element Method (AEM) and Finite Element Method (FEM). Within the scope of the study, the material models employed in the simulations, considering the limitations inherent in numerical modeling are discussed. The findings provide critical insights into the structural performance of PC utility poles under seismic loading and offer useful numerical tools for the development of retrofitting strategies in the near future.

2. Experimental program for seismic performance of PC utility poles

In this research, the experiment done by JR East using a cyclic loading system to investigate the seismic performance of PC utility poles was utilized for the simulation verifications [4]. The characteristics of the tested specimen, including the designed cracking bending

moment and bending moment capacity, were evaluated in accordance with JIS A5373:2016. [5].

2.1. Details of specimen and material properties

As shown in Figure 3, a 2650 mm PC utility pole which was cut from a full length of 12000 mm actual pole was embedded into the concrete footing ($1800 \times 1300 \times 600$ mm). The 25 mm gap between the PC pole and footing was filled by non-shrinkage mortar. The cross-section A-A in Figure 3 describes that there are 24 tension wires (TW) and 8 non-tension wires (NTW) arranged equally around the hollow circular section of 400 mm diameter pole. The material properties of the tested TWs and NTW were depicted in Table 1 while the 100 N/mm² compressive strength of concrete pole was the designed value.

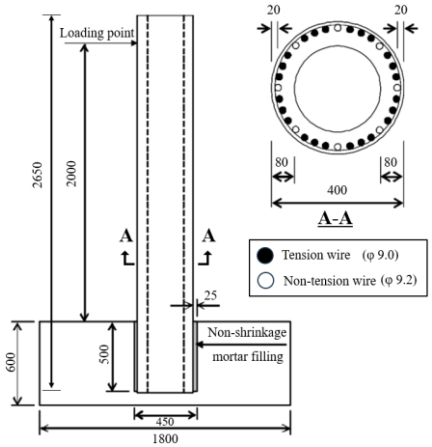

Figure 3. *Details of the tested PC utility pole [3]*

Table 1. *Material properties of the test*

Compressive strength of concrete pole (N/mm²)	Yield strength of wires	
	TW (N/mm²)	NTW (N/mm²)
100	1430	1206

2.2. Loading method and experimental results

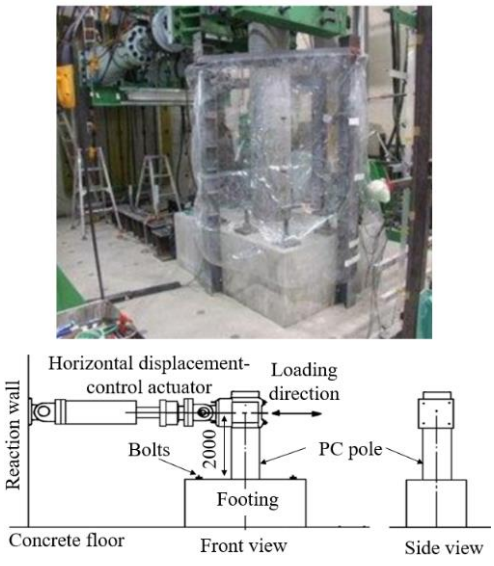

Figure 4. *Loading system applied to the specimen [3]*

The cyclic loading system is demonstrated in Figure 4. The horizontal displacement was controlled by an actuator at loading point (2000 mm from the footing). The footing was fixed to the concrete floor using 10 steel bolts (Figure 4). Since the yield displacement of a typical RC pole is about 1/200 rad, the loading step 1δ was conveniently set as 10 mm (1/200 rad), and thereafter 1δ increment displacement was applied until obtaining the design bending moment of 150 kN-m, corresponding to 75kN for horizontal load.

According to the report of Iwata *et al.*, the maximum load was reached at 6δ and the load dropped sharply at 7δ, after that the test was terminated at 8δ [4]. The load-displacement relationship of the specimen is described in Figure 5.

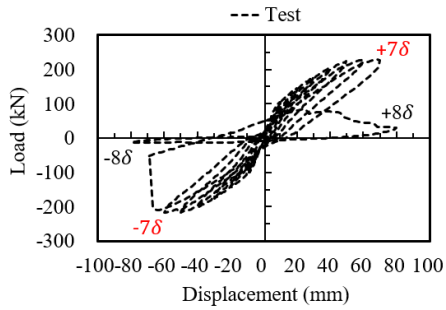

Figure 5. *Load-displacement relationship of the test [3]*

3. Verification of AEM simulation

3.1. Applied Element Method

AEM is an advanced numerical analysis technique first introduced by Meguro and Tagel-Din at the University of Tokyo in 1998 [6], based on the discrete cracking concept. In AEM, structures are represented as an assembly of small elements connected by normal and shear springs distributed across their entire surfaces. These springs simulate the stresses, strains, and deformations of a specific material volume [7]. When the springs between two adjacent elements fail, those elements can fully detach, enabling the method to accurately track crack initiation, propagation, and the load-deformation behavior of structures from initial stages to complete failure [6, 7].

As shown in Figure 6 and 7, the tested PC utility pole was successfully modeled using a commercial software named Extreme Loading for Structures (ELS) based on AEM.

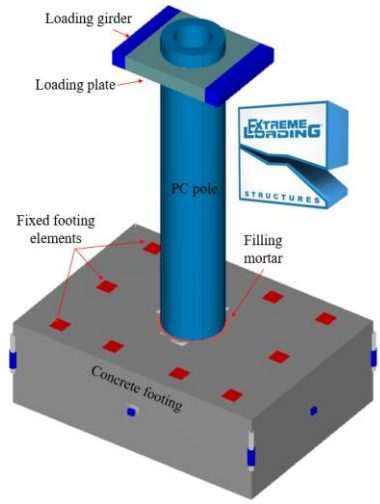

Figure 6. *3D AEM model for the PC utility pole*

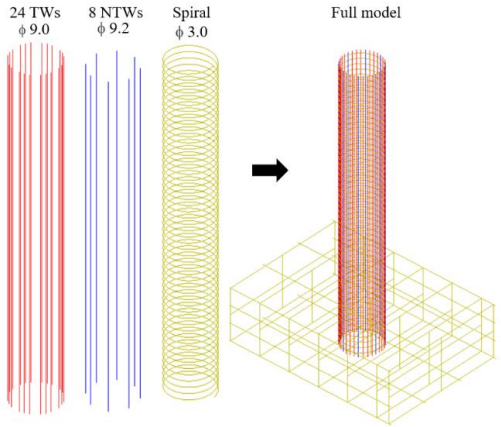

Figure 7. *AEM modeling of TWs, NTWs, spiral and reinforcement*

3.2. Material models in AEM

AEM employs fully nonlinear, path-dependent constitutive models. For concrete under compression, the elasto-plastic and fracture models of Maekawa and Okamura (1983) are applied [8]. In tension, a linear stress-strain relationship is used until the concrete springs crack, at which point the stresses drop to zero (Figure 8a).

According to Japanese standard specifications, the concrete with compressive strength larger than 55 N/mm² can be determined as high strength concrete [9]. In this experiment, the concrete compressive strength was about 100 N/mm², therefore, the stress-strain curve of high strength concrete with high failure softening factor (more brittle failure) was adopted, as described in Figure 8b. This failure softening behavior was also agreed with the findings by other researchers [9, 10]. As for the tensile strength and elastic modulus of high strength concrete model, the equations Eq.1 and 2 proposed by specifications were adopted [9]:

$$f_t' = 0.23 f_c'^{\frac{2}{3}} \quad \text{(Eq. 1)}$$

$$E_c = \left(3.7 + \frac{f_c' - 70}{100}\right) \times 10^4 \quad \text{(Eq. 2)}$$

where f_t'(N/mm²) denotes the tensile strength of concrete. f_c' (N/mm²) represents the compressive strength of concrete. E_c (N/mm²) reflects Young's modulus of concrete.

Reinforcement such as rebars in footing and spiral are modeled as bare bars for the envelope, with the internal loops based on the Ristic *et al.* model (Figure 8c) [11]. To model TWs, the designed force of 5.5 t per wire was applied to the appropriate 24 rebars ϕ 9.0 at the first stage before horizontal displacement was given.

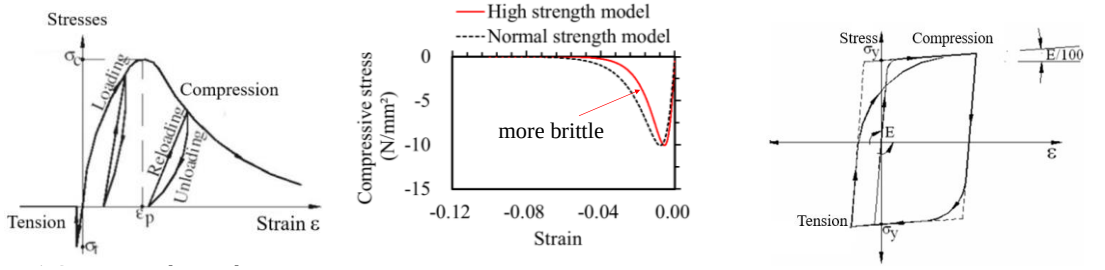

a) Concrete under axial stress *b) High strength concrete model* *c) Reinforcement under axial stress*

Figure 8. *Concrete and reinforcement material models in AEM*

The input mechanical properties of the materials in AEM model are listed in Table 2 and 3.

Table 2. *Material properties of concrete and mortar in AEM*

Properties	Concrete pole	Concrete footing	Mortar footing
Young's modulus (N/mm²)	37000	26700	37000
Compressive strength (N/mm²)	100	54.7	68.5
Tensile strength (N/mm²)	5.0	3.3	0.4

Table 3. *Material properties of TWs and NTWs in AEM*

Properties	TWs	NTWs
Young's modulus (N/mm²)	200000	200000
Yield strength (N/mm²)	1430	1206
Ultimate strength (N/mm²)	1600	1363

The loading stages in the AEM model are outlined in Table 4. In the first stage, only pretension force was applied to TWs, followed by horizontal displacements applied to the specimen in accordance with the experimental procedure.

Table 4. *Loading stages in the AEM model*

Stage	**Loading condition**	
1	Pretension of TWs	
2-18	Horizontal controlled displacements	
Stage	**Displacement (mm)**	**Amplitude (mm)**
1	0	0
2	10	10
3	-20	-10
4	30	20
5	-40	-20
6	50	30
7	-60	-30
8	70	40
9	-80	-40
10	90	50
11	-100	-50
12	110	60
13	-120	-60
14	130	70
15	-140	-70
16	150	80
17	-160	-80
18	80	0

3.3. AEM simulation results

Figure 9 illustrates the distribution of generated stresses along the length of TWs during loading process. After the application of the pretension force of 5.5 t, the tensile stress TWs reached approximately 800 N/mm² with an initial strain of 0.0039, as determined by the AEM model (Figure 9). These values closely align with the hand-calculated results of about 865 N/mm² and 0.004, respectively, indicating good agreement between the two methods. Additionally, the maximum compressive and tensile stresses in TWs reached 1330 N/mm² and 1470 N/mm², respectively, both of which are below the tested ultimate strength of 1600 N/mm² (Figure 9). Consequently, no rupture of TWs occurred during the experiment.

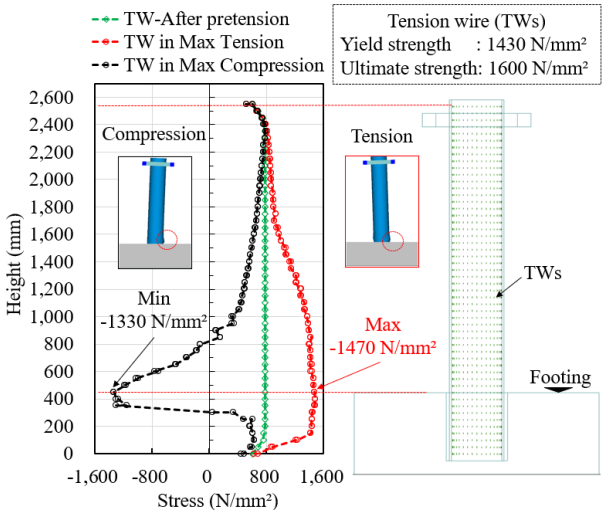

Figure 9. *Generated stresses in TWs during loading*

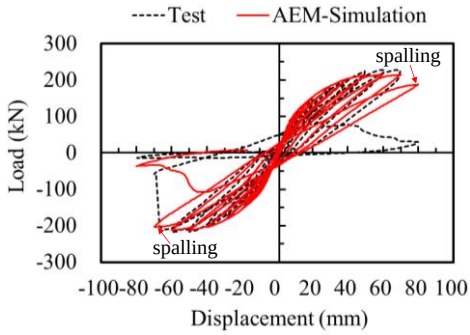

Figure 10. *Load-displacement relationship in AEM model*

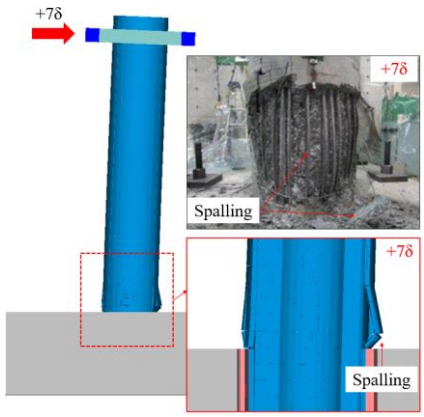

Figure 11. *Failure mode in AEM model*

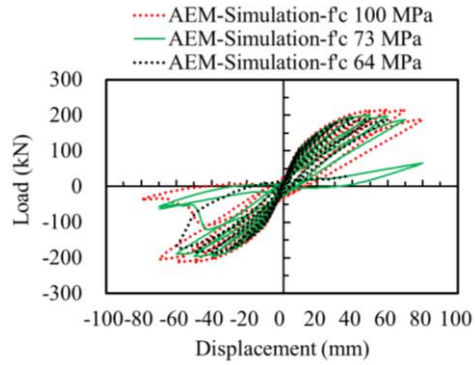

Figure 12. *The effect of concrete strength in AEM*

Figure 10 indicates that the load-displacement relationship obtained from AEM simulation closely matched the experimental results. In AEM model, the peak load reached 216 kN at the 6δ (60 mm) loading stage while in the experiment, a peak load of 228 kN was achieved at the same stage. Moreover, the crushing and spalling of concrete was also observed at the 7δ (70 mm) loading stage in the AEM model, followed by a sudden drop in loading capacity (Figure 11).

As shown in Figure 12, a parametric study was conducted to numerically investigate the effect of concrete compressive strength on the structural performance of the pole. According to several reports, the compressive strength of concrete pole varies from approximately 64 MPa to 100 MPa [4, 12]. The simulation results indicated that lower strength of concrete led to reduced load-bearing capacity, accompanied by the occurrence spalling failure at an earlier stage.

4. Verification of FEM simulation

4.1. Material models in FEM

The FEM analysis conducted in this study employs COM3 software, which enables nonlinear analysis of reinforced concrete structures based on an original constitutive law. In this software, each finite element is treated as a composite of both concrete and reinforcing bars [13].

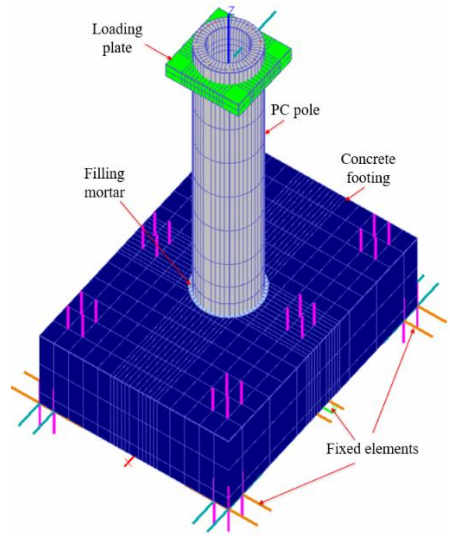

Figure 13. *3D FEM model for the PC utility pole*

The subject of the analysis in this study is the same PC utility pole specimen used in AEM analysis, as demonstrated in Figure 13. The reproduction analysis was conducted using cyclic loading tests performed on the specimen. The loading stages applied in the FEM model correspond to those outlined in Table 4. The input material properties are provided in Table 2 and 3.

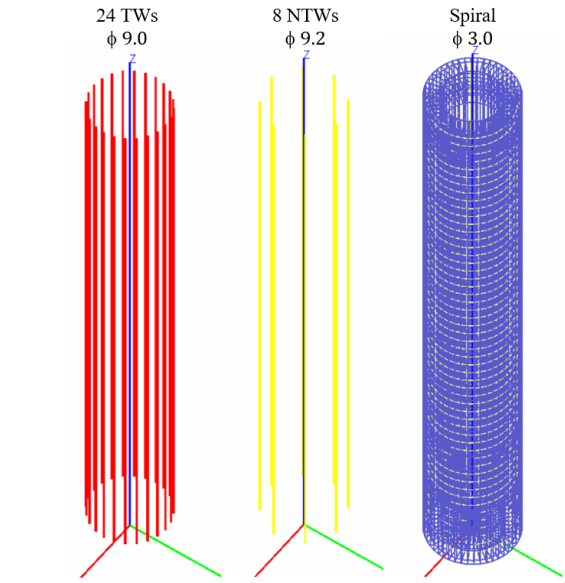

Figure 14. *FEM modeling of TWs, NTWs, spiral and reinforcement*

The structure under consideration is a prestressed concrete system, making the accurate representation of prestressing effects critical in the analysis. In the model presented here, the TWs were simulated using a prestress line element incorporated into the structural model. This element was positioned in accordance with the actual specimen, consisting of three tensioned wires followed by one non-tensioned wire, as shown in Figure 14. Pretension was introduced by applying an initial strain of 0.004 to each TW, which replicates the strain induced by the prestressing force of 5.5 t per wire.

4.2. FEM simulation results

As described in Figure 15, the load-displacement relationship obtained from FEM analysis corresponds relatively well to the experimental result, although the overall load range is smaller than that of the experimental result. However, explicit concrete failure, such as spalling, was not observed in the FEM model (Figure 16). To further investigate the stress state within the finite elements, the averaged stress-strain relationship of an element located just above the footing was extracted (Figure 16 and 17). It is important to note that the finite element, primarily representing concrete with rebar, was modeled using a smeared reinforcing bar approach in the constitutive law applied in this analysis. As a result, the stress-strain behavior of pure steel material cannot be directly obtained. Therefore, the average stress-strain relationship of the RC element is presented (Figure 17). In this relationship, the compressive stress reaches its compressive strength at approximately the 3δ (30 mm) loading stage, suggesting the onset of compression failure in the concrete. The absence of this failure phenomenon in the load-displacement relationship may be attributed to the gradual softening observed in the stress-strain behavior of the RC elements, which contrasts with the abrupt post-peak behavior typically seen in high-strength concrete during compression failure.

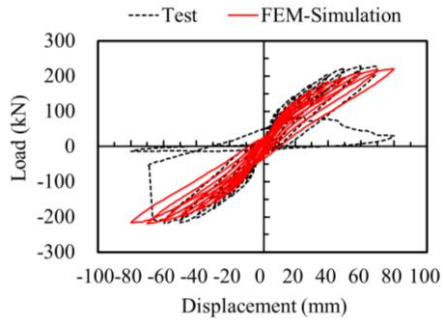

Figure 15. *Load-displacement relationship in FEM*

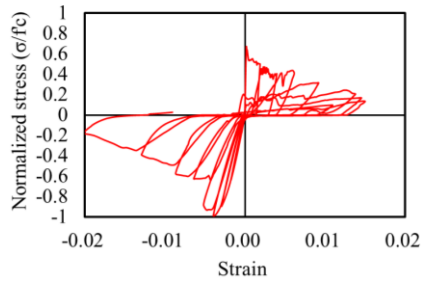

Figure 16. *Normalized stress-strain relationship in the extracted element*

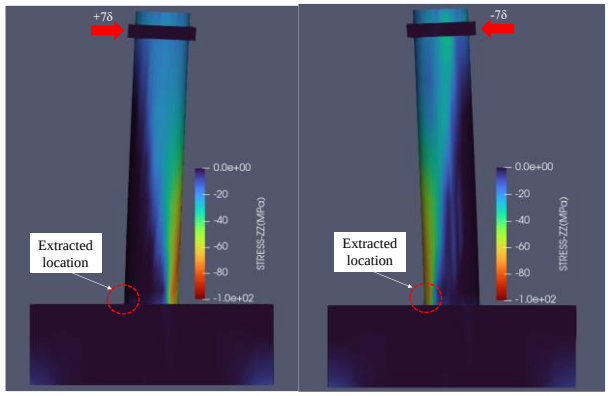

Figure 17. *Contour of concrete stress at 7δ (70mm) in FEM*

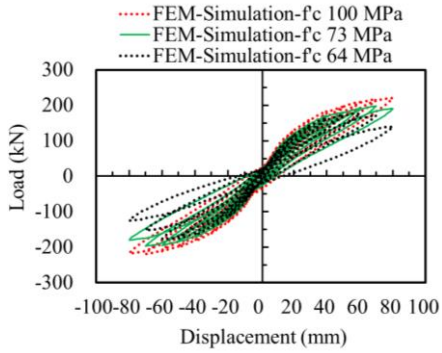

Figure 18. *The effect of concrete strength in FEM*

The effect of concrete compressive strength on the load-bearing capacity of the pole observed in FEM models agrees well with the results obtained from AEM models (Figure 12 and 18).

5. Conclusion

Based on the results from AEM and FEM simulations, several conclusions could be drawn:

(1) The AEM and FEM numerical models were successfully verified by experimental results with respect to the load-displacement relationship.

(2) The AEM model was capable of depicting concrete spalling in the compression zone, whereas this failure phenomenon was not captured by the FEM model.

(3) Both the AEM and FEM simulation results indicated that lower concrete strength led to a reduction in load-bearing capacity of the PC utility pole.

In the near future, various retrofitting methods to improve the performance of existing PC utility poles on Shinkansen viaducts in Japan will be developed and implemented. The utilization of reliable numerical tools, such as COM3 based on FEM and especially ELS based on AEM could prove significant advantages in understanding the contribution of retrofitting materials, failure mechanism and seismic performance of the retrofitted poles that may not be fully uncovered through experiments alone. Consequently, the need for extensive experimental work can be minimized, leading to substantial reduction in both cost and time.

REFERENCES

[1] S. Nozawa *et al.*,"Damage and restoration of the railway structures casued by the 2011 off the Pacific coast of Tohoku Earthquake (in Japanese)", *Geotechnical Engineering Journal*, vol. 7, no. 1, pp. 127-137, 2012.

[2] T. Sasaki *et al.*, "Earthquake damage to concrete utility poles for Shinkansen and remedial measure (in Japanese)", *Concrete Journal*, vol. 53, no. 7, pp. 622-628, 2015.

[3] *Design Standards for Railway Structures and Commentary: Seismic Design*, Railway Bureau, MLIT and Railway Technical Research Institute, 2012.

[4] M. Iwata, H. Kusano, and D. Tsukishima, "Seismic reinforcement method for PC utility poles (in Japanese)", in *Proceedings of the Japan Concrete Institute*, Japan, 2013, pp. 1087-1092.

[5] *Precast prestressed concrete products*, JIS A 5373, Japanese Industrial Standard, 2016.

[6] H. Tagel-Din, and K. Meguro, "Applied Element Method for Dynamic Large Deformation Analysis of Structures", *Doboku Gakkai Ronbunshu*, vol. 2000, no. 661, pp. 1-10, 2000.

[7] K. Meguro, and H. Tagel-Din, "AEM used for large displacement structure analysis", *Journal of Natural Disaster Science*, vol. 24, pp. 25-34, 2002.

[8] K. Maekawa, and H. Okamura, "The Deformational Behavior and Constitutive Equation of concrete Based on the Elasto-Plastic and Fracture Model", *Journal of the Faculty of Engineering, The University of Tokyo*, vol. 37, no. 2, pp. 253-328, 1983.

[9] *Standard Specifications for Concrete Structures - Design*, JSCE Guidelines for Concrete No. 16, 2007.

[10] M. P. Collins and D. Mitchell, *Prestressed concrete structures*, Prentice Hall, 1991.

[11] D. Ristic, "*Stress-Strain Based Modeling of Hysteretic Structures under Earthquake Induced Bending and Varying Axial Loads*", Reseach Report No. 86-ST-01, 1986.

[12] M. Onodera, *et al.*, "Experimental Study on Seismic Behavior of Reinforced PC Power Pole (in Japanese)", in *Proceedings of the Japan Concrete Institute*, Japan, 2024, pp. 181-186.

[13] K. Maekawa, H. Okamura, and A. Pimanmas, *Non-Linear Mechanics of Reinforced Concrete*, Taylor & Francis, 2003.